ClpP Hydrolyzes a Protein Substrate Processively in the Absence of the ClpA ATPase: Mechanistic Studies of ATP-Independent Proteolysis[†]

Laura D. Jennings,[‡] Desmond S. Lun,[§,||] Muriel Médard,[§] and Stuart Licht[‡,⊥,*]

Department of Chemistry and Laboratory for Information and Decision Systems, Massachusetts Institute of Technology, 77 Massachusetts Avenue, Cambridge, Massachusetts 02139

Received June 11, 2008; Revised Manuscript Received August 20, 2008

ABSTRACT: ATP-dependent proteases are processive, meaning that they degrade full-length proteins into small peptide products without releasing large intermediates along the reaction pathway. In the case of the bacterial ATP-dependent protease ClpAP, ATP hydrolysis by the ClpA component has been proposed to be required for processive proteolysis of full-length protein substrates. We present here data showing that in the absence of the ATPase subunit ClpA, the protease subunit ClpP can degrade full-length protein substrates processively, albeit at a greatly reduced rate. Moreover, the size distribution of peptide products from a ClpP-catalyzed digest is remarkably similar to the size distribution of products from a ClpAP-catalyzed digest. The ClpAP- and ClpP-generated peptide product size distributions are fitted well by a sum of multiple underlying Gaussian peaks with means at integral multiples of ~900 Da (7−8 amino acids). Our results are consistent with a mechanism in which ClpP controls product sizes by alternating between translocation in steps of 7−8 (±2−3) amino acid residues and proteolysis. On the structural and molecular level, the step size may be controlled by the spacing between the ClpP active sites, and processivity may be achieved by coupling peptide bond hydrolysis to the binding and release of substrate and products in the protease chamber.

Energy-dependent proteases are large molecular machines responsible for the intracellular degradation of misfolded and short-lived regulatory proteins. Members of this family include the eukaryotic 26S proteasome and the bacterial enzymes ClpAP, ClpXP, HslVU, Lon, and FtsH. In these systems, AAA+[1] (ATPases associated with a variety of cellular activities) components bind, unfold, and translocate protein substrates into barrel-shaped compartmental proteases where the substrates are hydrolyzed and released as peptide products (*1*−*4*). While much attention has been devoted to understanding how protein substrates are recognized, unfolded, and translocated by the ATPase component of energy-dependent proteases (*5, 6*), much remains to be learned about how proteolysis proceeds after the substrates reach the proteolytic chamber. In particular, the way that the ATPase and protease components may work together to maintain processivity is incompletely understood (*7*).

One way to study the proteolytic mechanism is to examine the size distribution of peptide products generated by these proteases. Different proteolytic mechanisms make distinct predictions about the shape of the product size distribution and its sensitivity to perturbations in enzymatic function (*8*). Size-exclusion chromatography allows the product size distribution to be estimated (*8*−*10*), with the caveat that the chromatogram reflects both the true size distribution and chromatographic factors that broaden the observed peaks (*11*). Previous work has shown that the size range of products generated by energy-dependent proteases spans a 10-fold range (from ~3 to ~30 residues). Interestingly, all ATP-dependent proteases for which product size has been characterized [including the 20S archaeal (*9*) and eukaryotic proteasomes (*10, 12*), the 26S proteasome (*10*) (which includes the protease subunits in the 20S proteasome, accessory ATPase subunits, and other regulatory subunits), ClpAP (*8*), HslVU (*13*), and Lon (*14, 15*)] share this size range of products. Furthermore, both ClpAP and the proteasome have been shown to generate approximately log-normal peptide product size distributions with a peak between 6 and 9 amino acids and a tail skewed toward longer products (*8*−*10*).

The similarity in the range of product sizes and in the shape of product size distributions suggests that all ATP-dependent proteases share a common proteolytic mechanism. However, this mechanism remains a matter of debate. The distance between protease active sites corresponds to 7−8 amino acids (*16*−*18*), matching the peak observed at this product length in both proteasome- and ClpAP-generated size distributions. This observation led to the hypothesis that the

[†] This work was supported by the Beckman Foundation and the Department of Chemistry.

* To whom correspondence should be addressed. Phone: (617) 452-3525. Fax: (617) 258-7847. E-mail: lichts@mit.edu.

[‡] MIT Department of Chemistry.

[§] Laboratory for Information and Decision Systems.

[⊥] Electrical Engineering and Computer Science Department.

[||] Current address: The Broad Institute of MIT and Harvard, 7 Cambridge Center, Cambridge, MA 02142.

[1] Abbreviations: AAA+, ATPase(s) associated with various cellular activities; HPLC, high-performance liquid chromatography; MALDI, matrix-assisted laser desorption ionization; ssrA, peptide with an AANDENYALAA sequence; HEPES, 4-(2-hydroxyethyl)-1-piperazineethanesulfonic acid; DTT, dithiothreitol; TFA, trifluoroacetic acid; BSA, bovine serum albumin; MMP-1, matrix metallopeptidase 1.

10.1021/bi801101p CCC: $40.75
Published on Web 10/08/2008

coordinated action of adjacent active sites controls peptide product sizes (i.e., the "molecular ruler" mechanism) (*16, 19*). However, a substantial fraction of both proteasomal (*9, 10*) and ClpAP (*8*) products are significantly longer or shorter than 7−8 amino acids, contrary to the prediction of the molecular ruler mechanism. Furthermore, both proteasome- and ClpAP-generated peptide product size distributions are unaltered by partial inactivation of up to 70% of the active sites (*8, 10*), in contrast to the molecular ruler mechanism, which predicts that partial inactivation will increase the average product size.

Alternatives to the molecular ruler mechanism have been proposed. For both the proteasome and ClpP, the action of product exit pores as a filter has been proposed to account for product size control. This "filter" mechanism postulates that once a substrate enters the chamber, proteolysis continues randomly until the peptide products are small enough to diffuse out of the chamber (*10, 18*). For ClpAP, we have proposed a mechanism in which alternation between translocation and proteolysis controls product sizes. In this mechanism, product sizes are independent of both the proteolysis rate and the translocation rate, consistent with experimental observations (*8*).

All energy-dependent proteases characterized to date are processive, meaning that they completely degrade protein substrates into small peptides without the release of large intermediates (*15, 20*−*22*). This feature is necessary for product size control in all of the proteolytic mechanisms that have been proposed. Furthermore, the specific mechanism of processive proteolysis is expected to influence the distribution of product sizes produced, but it is not yet clear how processivity is achieved in these systems. Surprisingly, the ATPase component is not always necessary for processivity. For example, the 20S proteasome can degrade full-length proteins into small peptide products [of the same size distribution as that generated by the ATPase-incorporating 26S proteasome (*10*)] without the aid of an ATPase component (*9, 10, 12*). However, for bacterial energy-dependent proteases, it has generally been proposed that the ATPase component is necessary for processive degradation of full-length proteins. While ClpP has been shown to degrade large polypeptides (up to 30 amino acids) processively, the enzyme has not been shown to degrade (processively or otherwise) full-length proteins in the absence of a partner ATPase (*20*). The Lon protease has been shown to degrade a full-length protein to a small extent in the absence of ATP, but the only peptides detected were from the terminal regions of the substrate protein, suggesting that this ATP-independent proteolysis is not processive (*14*).

The mechanism for ATP-independent processive proteolysis is not yet clear. One possibility is that peptide bond hydrolysis provides the driving force for processivity. This reaction is exergonic (*23*) and could drive processive proteolysis either through a power stroke or via a ratchet mechanism. Peptide bond hydrolysis has been shown previously to drive processive movement of activated collagenase (MMP-1) on collagen fibrils. Processivity in this system seems to be maintained via a Brownian ratchet mechanism, with biased diffusion of the collagenase enzyme on collagen fibrils fueled by proteolysis (*24*). A similar proteolysis-driven mechanism might account for the ATP-independent processivity observed with the 20S proteasome.

Given the apparent mechanistic similarities between the proteasome and ClpAP, it is surprising that processive proteolysis of large protein substrates by ClpAP appears to have an absolute requirement for ATP hydrolysis, while a similar reaction can be catalyzed by the 20S proteasome without concomitant ATP hydrolysis. However, since previous work did not put a lower limit on the rate of ClpP-catalyzed degradation of large protein substrates (*20*), one possibility is that ClpP alone does catalyze processive proteolysis, but at a rate lower than the limit of detection of previous experiments. In that case, the mechanistic similarities between the proteasome and ClpAP would extend to ATP-independent processive cleavage of protein substrates.

In this work, we investigate two questions related to ClpAP-catalyzed processive proteolysis. The first is whether ClpA is required for processive proteolysis of casein, a natively unfolded substrate. The results indicate that, contrary to what might have been predicted on the basis of previous work, the protease subunit ClpP can degrade casein processively in the absence of ClpA, albeit at a greatly reduced rate (an ~2000-fold rate decrease). This observation leads to the second question, which is how the product size distribution of ClpP products compares to the size distribution of ClpAP products. We show that the size distribution of peptide products from a ClpP-catalyzed digest is remarkably similar to the size distribution of products from a ClpAP-catalyzed digest. These results indicate that ClpP by itself can carry out processive proteolysis and control the product size distribution. Quantitative analysis of the product size distributions provides further mechanistic details. A deconvolution algorithm (*11*) is applied to the size-exclusion chromatograms to extract the true size distributions from underlying chromatographic factors. These deconvolved size distributions quantitatively fulfill the predictions of a mechanism in which ClpP translocates protein substrates in steps of 7−8 amino acids (±2−3 amino acids) and partitions after each step between another translocation step and proteolysis. The physical basis for this stepping mechanism is not yet clear, but we propose a model in which the step size is controlled by the spacing between the active sites and binding and release of the substrate and products in the protease chamber are coupled to peptide bond hydrolysis.

MATERIALS AND METHODS

Protein Purification. ClpA, ClpP-His_6, and GFP-ssrA were purified as described previously (*8, 25*−*27*). ClpPS97A-His_6 was purified from SG1146GaBL21(DE3) cells (a *clpp*$^-$ strain) in the same way as ClpP-His_6. ClpP-His_6 was purified from either DH5α cells or S1146GaBL21(DE3) cells; the two preparations had comparable activity (see Figure S1 of the Supporting Information). α-Casein and chymotrypsin were purchased from Sigma.

Reductive Methylation of Substrate Proteins. To prevent reaction of fluorescamine with lysine side chains, reductive methylation of GFP-ssrA and α-casein was carried out using formaldehyde and sodium cyanoborohydride as previously described (*8, 28*). All degradation assays were performed using methylated substrates. However, for the sake of simplicity, methylated GFP-ssrA and methylated α-casein are here named "GFP-ssrA" and "casein", respectively.

Processivity Measurements. Casein was degraded by ClpP or ClpPS97A in buffer containing 50 mM HEPES (pH 7.5), 20 mM $MgCl_2$, 100 mM NaCl, 10% glycerol, 0.5 mM DTT, 100 μM casein, and 4 μM wild-type $ClpP_{14}$ or $ClpPS97A_{14}$. The reactions were allowed to proceed for 24 h at 37 °C. Chymotrypsin-catalyzed degradation of casein was performed under the same conditions, except 0.133 μg/mL chymotrypsin was used in place of ClpP, and the reaction was allowed to proceed for 2 h. Aliquots of the reaction mixtures were taken at various time points and the reactions in each aliquot quenched by the addition of an equal volume of 7.4 M Gu-HCl. Peptide product formation was assessed using fluorescamine (*29*), which forms a fluorescent product upon reaction with primary amines. Each quenched sample (10 μL) was mixed with 100 μL of 100 mM HEPES (pH 6.8) and 50 μL of 0.3 mg/mL fluorescamine in acetone (freshly prepared before use). After 7.5 min, the fluorescence was measured (excitation at 370 nm, emission at 510 nm) using a microplate spectrofluorimeter (Molecular Devices Spectramax Gemini XS). To convert relative fluorescence units into peptide product concentration, a standard curve was prepared using the ssrA peptide (AANDENYALAA) derivatized with fluorescamine in the same way as the digested peptides. To assess casein degradation, each quenched sample was loaded onto an HPLC reverse-phase C18 analytical column (Jupiter, 150 mm × 4.60 mm, 5 μm, Phenomenex). ClpP digests were eluted with the following gradient program at a flow rate of 1 mL/min: isocratic elution with 95% solvent A (0.1% TFA in water) and 5% solvent B (0.1% TFA in acetonitrile) for 5 min, a linear gradient from 95% A and 5% B to 80% A and 20% B for 5 min, and a linear gradient from 80% A and 20% B to 30% A and 70% B for 30 min. For chymotrypsin digests, the following gradient program was used: isocratic elution with 95% A and 5% B for 5 min, a linear gradient from 95% A and 5% B to 80% A and 20% B for 15 min, and a linear gradient from 80% A and 20% B to 50% A and 50% B for 60 min. Casein eluted as a single peak that was well separated from product and protease peaks and was detected by absorbance at 280 nm. Experiments were performed in triplicate.

Digestion of Casein and GFP-ssrA by ClpAP or ClpP for Size-Exclusion Chromatography Studies. Proteolysis of GFP-ssrA by ClpAP was performed in a reaction mixture containing 50 mM HEPES (pH 7.5), 30 mM $MgCl_2$, 300 mM NaCl, 10% glycerol, 0.5 mM DTT, 25 μM GFP-ssrA, 50 nM $ClpP_{14}$, 100 nM $ClpA_6$, 10 mM ATP, and an ATP regenerating system consisting of 30 mM phosphocreatine and 0.05 unit/μL creatine phosphokinase (from rabbit muscle, Sigma). The total reaction volume was 300 μL. The reaction was allowed to proceed for 2 h at 37 °C and was quenched by boiling. For proteolysis of casein by ClpAP, the same reaction conditions were used except that 20 mM $MgCl_2$ and 100 mM NaCl were present in the buffer, and $ClpP_{14}$ (100 nM) and $ClpA_6$ (200 nM) were used to degrade casein (25 μM). The reaction was allowed to proceed for 45 min at 37 °C, at which point the reaction was quenched by boiling. Casein was degraded by ClpP in a reaction mixture containing 50 mM HEPES (pH 7.5), 20 mM $MgCl_2$, 100 mM NaCl, 10% glycerol, 0.5 mM DTT, 50 μM casein, and 5.5 μM wild-type $ClpP_{14}$. These reactions were allowed to proceed for 24 h at 37 °C, followed by quenching via boiling. In each case, controls were performed in the absence of enzyme, and the experiments were performed in triplicate.

Size-Exclusion Chromatography of Peptide Products. Peptide products were derivatized with fluorescamine prior to chromatography to enable online detection. Following desalting with a reverse-phase cartridge (Sep-Pak C18, Waters) and concentration by centrifugal evaporation, peptide products were resuspended in 400 μL of 100 mM HEPES (pH 6.8); 3−20 μL of peptide products [diluted to a total volume of 20 μL with 100 mM HEPES (pH 6.8)] was then added to 10 μL of 0.3 mg/mL fluorescamine (in acetone, freshly prepared before use). After 1 min, 30 μL of water was added to the reaction mixture, and the sample was loaded immediately onto the size-exclusion column (*12*). Size-exclusion HPLC was performed using a polyhydroxyethyl aspartamide column (200 mm × 4.6 mm, PolyLC) (*30*). The mobile phase consisted of 200 mM sodium sulfate, 5 mM potassium phosphate, and 25% acetonitrile (pH 3.0, adjusted with phosphoric acid), and the flow rate was 0.125 mL/min. Peptides were detected using an online fluorescence detector (excitation at 380 nm, emission at 510 nm). To determine the apparent molecular masses of the peptides that eluted, the column was calibrated with 5−12 commercially available standard peptides in the 400−2500 Da range that had been derivatized with fluorescamine in the same way as the digest peptides.

Matrix-Assisted Laser Desorption Ionization (MALDI) Mass Spectrometry. Peptide products were desalted using a reverse-phase cartridge (Sep-Pak C18, Waters) and concentrated by centrifugal evaporation if necessary. One microliter (~100 pmol) was spotted onto a MALDI sample plate and allowed to dry; thereafter, 0.6 μL of matrix (15 mg/mL α-cyano-4-hydroxycinnamic acid in 80% acetonitrile) was spotted on top of the peptides. The MALDI spectra were recorded on a PerSeptive Biosystems Voyager-DE STR instrument in positive ion mode. The instrument was calibrated each time before use. To count the number of peptides in each spectrum, the background was first corrected using the MATLAB (MathWorks, Natick, MA) command msbackadj. A noise cutoff was set (at $\mu + 2.5\sigma$ ion counts, where μ is the mean ion count of the background signal and σ the standard deviation of the background signal), and all peaks above this threshold were counted as peptide products.

Deconvolution of Size-Exclusion Chromatograms. The average peak shape and standard deviation in peak width for single peptides were determined from measurements of 12 standard peptides. A random-restart gradient algorithm was used to generate a maximum likelihood estimate for the size distribution given the observed chromatogram and the properties of peaks arising from single peptides (*11*). The computation was implemented in MATLAB 7.1 (scripts available on request).

RESULTS

Degradation by ClpP Is Processive. To understand the mechanism of product size control by ClpAP, we must know whether processive proteolysis by this enzyme is ClpA-dependent. Previous studies have shown that ClpP alone can processively degrade large (up to 30 amino acids) peptide substrates (*20*), but to the best of our knowledge, ClpP-catalyzed degradation of a full-length protein in the absence

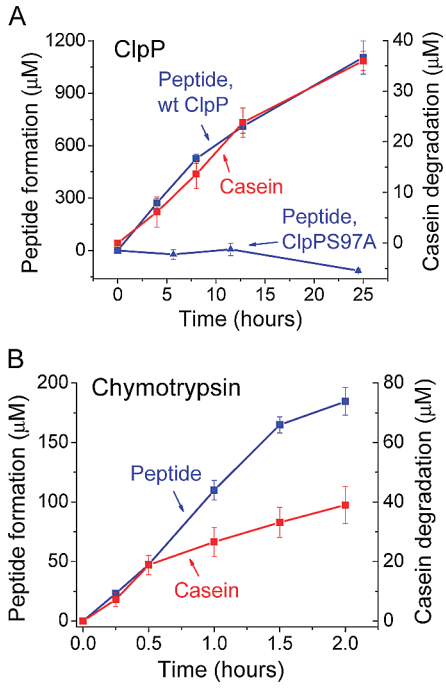

FIGURE 1: ClpP alone can processively degrade a protein substrate. Shown are the (A) ClpP-catalyzed and (B) chymotrypsin-catalyzed degradation kinetics of casein. Peptide product formation (blue) is shown on the left *y*-axis, and loss of intact casein (red) is shown on the right *y*-axis. To show that degradation is ClpP-dependent, we assessed peptide product formation with the ClpP S97A active site mutant (blue triangles, panel A). Error bars represent the standard error of the mean of three independent trials.

of ClpA or ClpX has not previously been reported. We therefore assessed the ability of ClpP alone to carry out processive degradation of a full-length protein substrate.

To facilitate digestion of a full-length protein in the absence of an ATPase, we used as a substrate the natively unfolded protein α-casein (methylated at the lysine side chains to prevent reaction with fluorescamine), and we allowed the degradation reaction to proceed for 24 h. We then assessed degradation by quantifying the formation of peptide products via their fluorescamine reactivity (*29*). The degradation rate was ~2000-fold slower for ClpP alone than for ClpAP; a control digestion using the catalytically inactive S97A ClpP mutant (*31*) showed no measurable activity for this mutant, indicating that the proteolysis observed with wild-type ClpP was due to the purified enzyme rather than a contaminating protease (Figure 1A). To assess processivity, we measured the ratio of total product formation to casein degradation over time. If degradation is processive, the ratio *n* of peptide products formed to intact casein degraded should remain constant over time, because formation of *n* equivalents of new peptide products will require degradation of 1 equiv of casein. However, if degradation is nonprocessive, the ratio of peptide products formed versus casein molecules degraded will increase over time; partially degraded intermediates released at early extents of the reaction will become substrates for the enzyme, leading to the formation of new peptide products without the degradation of any additional intact casein (*21*).

The results show that the ratio of peptide products to casein molecules degraded remains constant during ClpP-catalyzed degradation, indicating that degradation by ClpP is processive (Figure 1A). Furthermore, since the size distribution of ClpP-generated products shows a dominant peak around 7−8 amino acids, processive degradation of an ~250-amino acid substrate such as casein is expected to yield ~30 peptides per casein molecule degraded, even at low extents of reaction. Our results indicate that the ratio of peptide products formed to casein molecules degraded is ~30 throughout the reaction, consistent with processivity. In contrast, in control studies with the nonprocessive enzyme chymotrypsin, the ratio of peptide products to casein molecules increases over time from 2 at an ~10% extent of reaction to 5 at an ~40% extent of reaction, as expected for a nonprocessive enzyme (Figure 1B). These data thus support the surprising conclusion that although in the absence of ClpA, ClpP-catalyzed degradation of a full-length unfolded protein substrate is slow, ClpA is not needed to achieve processive proteolysis of this substrate.

Size-Exclusion Chromatography of ClpAP Products. To improve our understanding of the role of ClpA in determining the size distribution of ClpAP-generated peptide products, we analyzed ClpAP's peptide products using size-exclusion chromatography. The size-exclusion chromatogram of ClpAP-generated peptide products was previously characterized using postcolumn fluorescamine derivatization to quantify the peptide products (*8*). This technique produced a chromatogram with a resolution that was high enough to resolve the dominant features (such as a peak at 6−8 amino acids and the skewness of the chromatogram toward larger peptide sizes). However, the necessity of pooling fractions for a postcolumn assay limited the resolution of the data, leaving open the possibility that the size distribution had additional unresolved features. To generate a higher-resolution chromatogram, we derivatized ClpAP-generated peptide products with fluorescamine prior to size-exclusion chromatography (*12*) and detected the products using an online fluorimeter. We used as substrates α-casein and GFP-ssrA. Despite the distinct properties of these two substrates (in fold and amino acid composition), the high-resolution size-exclusion chromatograms of both sets of peptide products are remarkably similar. As expected, both chromatograms show a peak at ~800−900 Da (~7−8 amino acids). However, in both cases, the higher-resolution chromatogram reveals a previously undetected shoulder peak around 1600−1800 Da (~14−16 amino acids) and a tail skewed toward longer products (Figure 2 and Figure S2 of the Supporting Information).

Size-Exclusion Chromatograms of ClpP Products. To help determine how processive proteolysis occurs without substrate translocation by ClpA, we characterized the size distributions of ClpP-generated peptide products in the absence of ClpA. As in the processivity studies, we used casein as a substrate and allowed the reaction to proceed for 24 h. The size distribution of ClpP-generated peptide products is qualitatively different from the distribution observed for ClpAP products. It shares the same dominant peak around 800−900 Da and a shoulder peak around 1700 Da but has a significantly shorter tail (products of >2500 Da constitute ~3% of the ClpP-derived size distribution, while products of >2500 Da constitute ~10% of the ClpAP products; see Figure 2).

Validation of MALDI MS as a Technique for Measuring the Number Distributions of Peptide Product Sizes. The size-exclusion data indicate that the size distribution of ClpP-generated peptide products has an overall shape similar to but a range narrower than that derived from ClpAP. To test

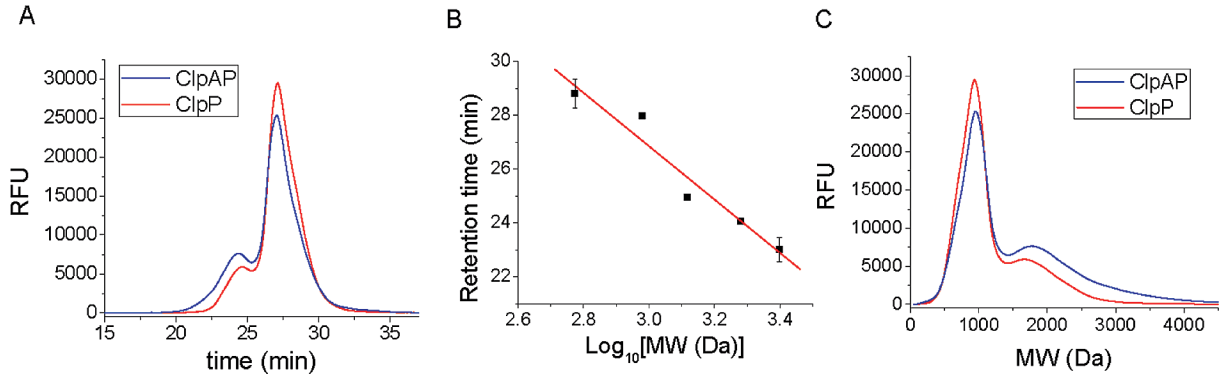

FIGURE 2: Size-exclusion chromatograms. (A) Size-exclusion chromatograms of ClpAP- and ClpP-derived peptide products from casein digests. Shown are the average traces of three independent trials. (B) Calibration curve used to convert retention time to molecular mass. Standard peptides were chromatographed in duplicate or triplicate; error bars represent standard deviations. (C) Size-exclusion chromatograms in which the *x*-axis has been converted from retention time to molecular mass using the calibration curve shown in panel B.

this conclusion with an independent method, we used MALDI mass spectrometry to determine the range of peptide product sizes. We digested casein with ClpAP or ClpP and obtained the MALDI mass spectra of the resulting peptide products. Because ionization efficiencies differ for different peptides, ion intensities in MALDI mass spectra cannot be used to compare amounts of individual peptides. However, counting the number of distinct peaks in a defined size window gives the number distribution of peptide products, which is useful for determining the mass range of peptide products from a given digest.

To assess the utility of MALDI mass spectra in determining number distributions of peptide product sizes, we obtained MALDI-derived number distributions of peptide products from both tryptic and chymotryptic digests. These experimental distributions were compared to the expected number distributions, which were calculated using the well-defined residue specificities of the proteases. To obtain a sufficient number of distinct peptides for statistical analysis, we digested bovine serum albumin (BSA) and ClpA together as a mixture and analyzed the peptide products by MALDI. A histogram plotting the number of peptides detected versus the molecular mass was compared to the expected histograms for both a chymotryptic digest and a tryptic digest of the two proteins (Figure S3 of the Supporting Information). A χ^2 analysis revealed that the expected chymotrypsin distribution is a good fit to the observed chymotrypsin distribution ($0.95 > p > 0.90$), and the expected trypsin distribution fits the observed trypsin distribution ($p \approx 0.9$). However, the expected chymotrypsin distribution does not fit the observed trypsin distribution ($p < 0.005$), nor does the expected trypsin distribution fit the observed chymotrypsin distribution ($p < 0.025$). Moreover, the number of peptides detected using MALDI was approximately the same as the number of peptides expected (for trypsin, 81 are expected and 81 ± 1 are found; for chymotrypsin, 61 are expected and 70 ± 4 are found). These results indicate that MALDI mass spectrometry allows accurate measurement of the product number distribution for two proteases with distinct specificities and suggest that this technique will be generally useful in determining number distributions. Use of this technique in combination with liquid chromatography and tandem mass spectrometry might be useful in measuring both substrate specificity (via product identification) and product number distributions.

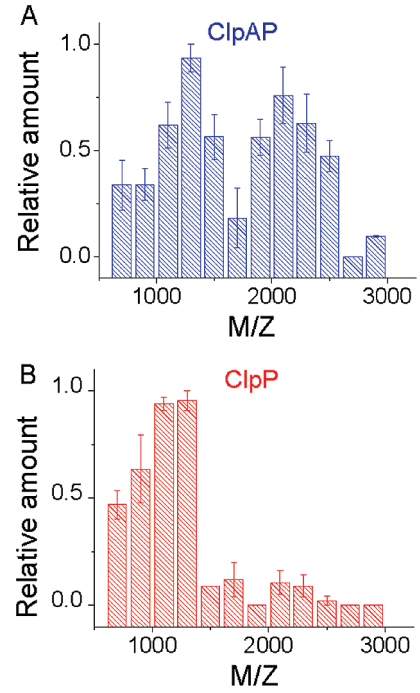

FIGURE 3: MALDI-derived number distributions. Shown are the (A) ClpAP-generated and (B) ClpP-generated peptide product number distributions from casein digests. Error bars represent the standard error of the mean of three independent trials. Because singly charged ions dominate MALDI spectra (*46*), *m*/*z* approximates molecular mass (daltons).

MALDI Number Distributions of ClpAP and ClpP Digests. MALDI was used to determine the number distribution of peptide products generated in ClpAP and ClpP digests of casein. The distributions follow the same pattern observed with size-exclusion chromatography. The distribution obtained from ClpAP digests of casein contains a peak at 1100−1300 Da and a second peak at 2100−2300 Da (Figure 3A). However, the distribution obtained from a ClpP digest of casein shows only a peak at 1100−1300 Da; the peak at 2100−2300 Da observed in the ClpAP distribution is absent from the ClpP-derived distribution (Figure 3B). These data provide additional evidence showing that the size distribution of ClpP-generated products has an overall shape similar to but a range narrower than that of the size distribution of ClpAP products.

Fitting Multiple Gaussian Peaks to the Size-Exclusion Chromatograms. Because ClpP-catalyzed casein degradation

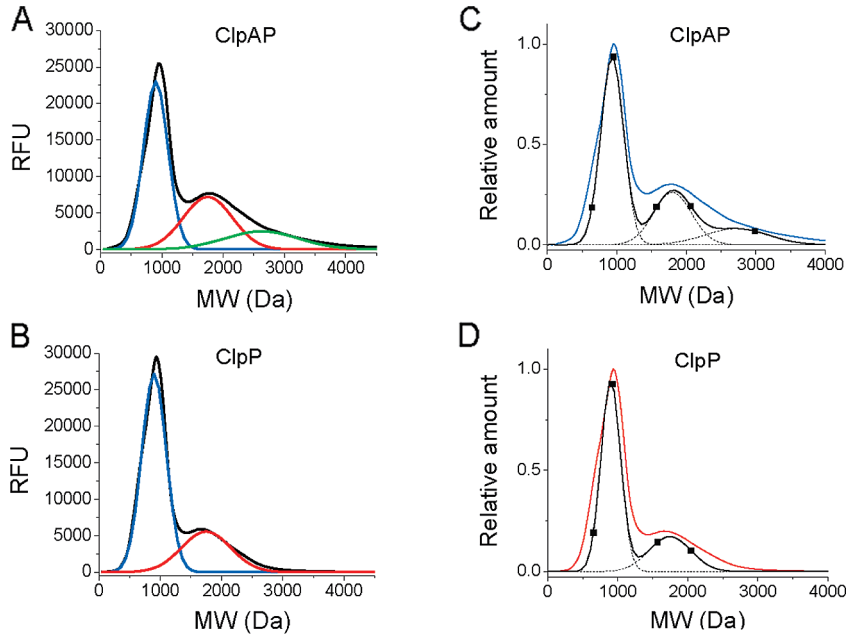

FIGURE 4: Fits of the size-exclusion chromatograms and the deconvolved size distributions to sums of Gaussians. The size-exclusion chromatograms of (A and C) ClpAP-derived and (B and D) ClpP-derived peptide products (from casein digests) were fitted to sums of underlying Gaussian components. The first component is colored blue, the second red, and the third green. In panels C and D, the raw chromatograms are shown as colored traces, the deconvolved size distributions are shown as black squares, and the fits of the deconvolved distributions to sums of Gaussians are shown as black lines. The underlying Gaussian components are shown as black dotted lines.

is also processive in the absence of ClpA, comparing the ClpAP size distribution with that of ClpP alone may reveal mechanistic similarities or differences between ClpA-assisted and ClpA-independent processive proteolysis. To compare the size distributions, we fitted the size-exclusion chromatograms to sums of Gaussian components (Figure 4). The first and largest amplitude component is at ~900 Da. The second component, both broader and smaller in amplitude than the first, is at ~1750 Da and is the major contributor to the shoulder in the chromatogram. A third component, even broader and smaller than the first two, is needed to account for the tail observed in the ClpAP distribution (Figure 4A). In contrast, this third component is not needed to account for the ClpP size distribution (Figure 4B).

Deconvolution of the Size-Exclusion Chromatogram. The size-exclusion chromatograms are determined by both the true size distribution and chromatographic features that are independent of the size distribution, such as peak broadening and tailing. To derive mechanistic conclusions from the size-exclusion data, it would be useful to deconvolve the true size distribution from these chromatographic factors. We therefore developed a deconvolution algorithm for the size-exclusion chromatograms. First, we recorded chromatograms for 12 standard peptides with molecular masses varying from ~400 to ~2500 Da. These chromatograms provided an average peak shape function, the mean peak width of a single peptide, and an estimate for the uncertainty in peak width. Using these values, we carried out a maximum likelihood estimation of the peptide size distributions underlying the observed chromatograms; the method is described in full detail in a separate work (*11*). A standard statistical criterion for model discrimination, the Akaike information criterion (*32*), was used to determine the most probable number of components underlying the chromatograms. This criterion provides an unbiased estimate of the information divergence between the true probability distribution of a system and the estimated distribution derived from a model.

Table 1: Results from Fitting ClpAP and ClpP Deconvolved Size Distributions to a Sum of Gaussian Components

	μ (Da)	σ (Da)	relative amplitude (%)	average peptide size (Da)
ClpAP				
component 1	931	324	58	1408
component 2	1801	545	27	
component 3	2724	905	14	
ClpP				
component 1	899	277	72	1136
component 2	1745	599	28	
component 3	–	–	–	

The deconvolved size distributions are qualitatively similar in breadth and skewness to the original chromatograms (Figure 4C,D). This observation shows that the dominant contributor to the breadth of the chromatograms is the true size distribution rather than chromatographic factors. It also indicates that the skewness toward longer products observed in the raw chromatograms is not an artifact of chromatography but rather a feature of the actual product size distributions.

Fitting the Deconvolved Size Distributions. The deconvolved size distributions for ClpAP and ClpP peptide products were fitted to sums of Gaussians. As found for the direct fits to the size-exclusion chromatograms, three Gaussian components were needed to fit the ClpAP deconvolved size distribution, but only two components were necessary to fit the ClpP size distribution (Figure 4C,D). Three parameters were determined for each Gaussian component: the mean, the standard deviation, and the amplitude (Table 1). In the context of the proposed mechanism for processive proteolysis (Figure 5), these three parameters can be used to determine the translocation step size, the variability in step size, and the probability that the substrate is cleaved

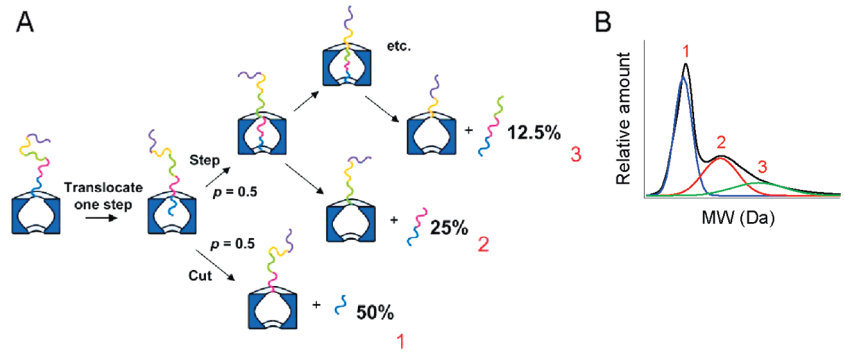

FIGURE 5: Proposed stepwise mechanism for translocation and proteolysis by ClpP. (A) Following binding of the unfolded protein substrate, ClpP translocates this substrate one step (equal to 7−8 amino acids). Following this step, the enzyme partitions between taking another step and proteolysis. Proteolysis after one step results in a pool of peptides at the step size of the enzyme; proteolysis after two steps results in a pool of peptides at twice the step size, and proteolysis after three steps generates peptides at three times the step size. The partitioning ratio between stepping and proteolysis determines the relative amplitudes of the product pools. For example, a partitioning ratio of 50:50 (as shown) results in product pools with relative amplitudes of 50, 25, 12.5%, etc. (B) The mechanism in part A results in a size distribution composed of three Gaussian peaks.

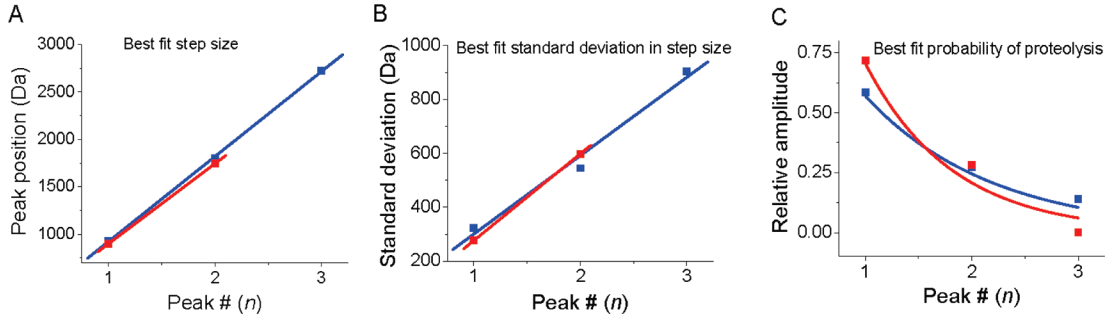

FIGURE 6: Fits of the deconvolved size distribution data to the predictions of the stepwise model: blue for ClpAP and red for ClpP. (A) The slope of peak position vs peak number gives a best-fit value for the step size of 900 ± 20 Da (7.6 ± 0.2 amino acids) and 845 Da (7.1 amino acids) for ClpAP and ClpP, respectively. (B) The slope of standard deviation vs peak number gives a best-fit standard deviation in the step size of 290 ± 40 Da (2.4 ± 0.3 amino acids) and 320 Da (2.7 amino acids) for ClpAP and ClpP, respectively. (C) Fitting the relative amplitudes of the underlying peaks to a geometric distribution [$f(n) = (1 - p)^{n-1}p$, where p is the probability of proteolysis and n the peak number] gives best-fit values for the probability of proteolysis of 0.57 ± 0.03 and 0.71 ± 0.06 for ClpAP and ClpP, respectively.

rather than taking a subsequent translocation step (Figure 6). The determination of the model parameters from the fits is described in the Discussion section.

DISCUSSION

ClpP Controls Processivity and Peptide Product Sizes. We present here data showing that ClpP in the absence of ClpA can degrade the full-length (~250-amino acid) natively unfolded protein, casein, albeit at a rate much slower than that of ClpAP (~2000-fold slower). Despite the slow rate of reaction, degradation by ClpP is processive, like ClpAP-catalyzed degradation. These surprising results indicate that ATP-driven translocation by ClpA is not necessary to achieve processive proteolysis of a full-length protein and suggest that ClpP alone can drive processive substrate translocation, albeit at a very slow rate.

Deconvolved size distributions of ClpAP- and ClpP-derived peptide products provide information about the roles of ClpA and ClpP in product size control. Each size distribution has a large peak at 800−900 Da (7−8 amino acids) and a second smaller peak at 1700−1800 Da (14−15 amino acids). In addition, the ClpAP distribution has a tail (comprising ~10% of the distribution) extending out to ~4000 Da; this tail is largely missing from the ClpP distribution. MALDI-derived number distributions confirm that the longest products present in the ClpAP distribution are not present in the ClpP distribution. Like the processivity data, these results indicate that, contrary to our previous hypothesis (*8*), the action of ClpA is not required to control product sizes. Instead, it appears that product sizes are controlled largely by ClpP.

ClpAP and ClpP Size Distributions Are Consistent with a Stepping Mechanism. Both the raw size-exclusion chromatograms and the deconvolved size distributions of ClpAP- and ClpP-derived peptide products can be fitted well with a sum of underlying Gaussian peaks. A size distribution composed of one or more Gaussian peaks is consistent with a mechanism in which ClpP-catalyzed deterministic translocation of the substrate into the protease chamber alternates with proteolysis at one or more of the ClpP active sites. In such a mechanism, if a translocation event is always followed by a proteolysis event, one Gaussian peak would be predicted in the size distribution. Furthermore, the mean of this Gaussian peak would reveal the average length of the substrate threaded into the active sites during each translocation event (termed the "step size" of the enzyme), while the standard deviation would reveal the variation in this step size. A size distribution composed of multiple peaks (as observed) could arise if the enzyme partitions between translocation and proteolysis, rather than cleaving the substrate after each translocation event. Therefore, a second peak in the size distribution would arise from partitioning

twice toward translocation before proteolysis, and a third peak would arise from partitioning three times toward translocation prior to proteolysis, etc. (Figure 5).

Obtaining Best-Fit Values for Step Size, Standard Deviation in Step Size, and Partitioning Ratio. Best-fit values for three parameters of the stepwise mechanistic model outlined in Figure 5 (the step size, the standard deviation in the step size, and the probability of translocation vs proteolysis) were obtained from fits of the ClpAP- and ClpP-derived deconvolved size distributions to sums of Gaussian components. These three parameters were determined from three predictions that the model makes about the properties of the product size distribution. First, the model predicts that the step size can be determined from the means (peak positions) of the underlying Gaussians. Specifically, the model predicts that the underlying components will be regularly spaced and that the spacing between the components will equal the translocation step size of the enzyme. For ClpAP- and ClpP-derived peptide product size distributions, the underlying Gaussian components are spaced ~800−900 Da (7−8 amino acids) apart. The best-fit slope of the peak position versus peak number gives a step size of 7−8 amino acids for both ClpAP and ClpP (Figure 6A).

In addition, the stepwise model (Figure 5) predicts that the standard deviation in the translocation step size can be determined from the standard deviation of the underlying Gaussian components. In this model, the standard deviations of the underlying Gaussians will increase linearly with each component. When some intrinsic variation in size is associated with each translocation step, taking two translocation steps before proteolysis will lead to a doubling of the associated variability, taking three translocation steps before proteolysis will triple the variability, etc. As predicted by the model, the observed standard deviations of the underlying Gaussian components of both the ClpAP- and ClpP-derived distributions increase linearly with peak position, and the slope of the standard deviation versus peak number gives a best-fit value for the standard deviation in the step size of 2−3 amino acids for both ClpAP and ClpP (Figure 6B).

Finally, the stepwise mechanism outlined in Figure 5 predicts that the partitioning ratio between proteolysis and further translocation can be determined from the amplitudes of the underlying Gaussian components. Specifically, the proposed mechanism predicts that the amplitudes of the underlying Gaussian components will decrease according to a geometric distribution (*33*) [$f(n) = (1 - p)^{n-1}p$, where p is the probability of proteolysis and n the peak number]. This relationship is observed in the data, and fitting the underlying peak amplitudes to a geometric distribution gives a best-fit value for the probability of proteolysis versus translocation for both enzyme conditions. The best-fit probabilities of proteolysis are 0.57 and 0.71 for ClpAP and ClpP, respectively (Figure 6C). This slight increase in partitioning toward proteolysis for the ClpP-catalyzed reaction versus the ClpAP-catalyzed reaction is consistent with the deficiency of longer ClpP products observed by both size-exclusion chromatography and MALDI mass spectrometry. The small differences between these distributions are somewhat difficult to interpret mechanistically. The similarities, however, are striking. Although the proteolytic rate is slowed tremendously by the absence of ClpA, the lack of an ATPase does not prevent processive proteolysis in discrete steps.

Alternative Mechanisms for Product Size Control. The size distribution data are inconsistent with two alternative mechanisms for peptide product formation. Product size might be determined by a filter mechanism, in which larger products cannot diffuse out of the complex and are therefore recleaved until they are small enough to escape (*10, 18*). However, it is difficult to reconcile this mechanism with the observation that the peaks in the product size distribution are approximately Gaussian. A structural pore that acts as a filter would be expected to admit smaller peptides preferentially, skewing the size distribution toward smaller products. In addition, since exit through equatorial pores appears to be the dominant mode of peptide release for ClpP (*34, 35*), the filter mechanism seems most consistent with only a single peak in the product size distribution (corresponding to the equatorial pore size), in contrast to the observation of up to three peaks experimentally. Another alternative mechanism is the molecular ruler, in which cleavage at two adjacent active sites produces products at a size equivalent to the intersite distance (*19*). However, to yield large fractions of product at the size corresponding to the intersite distance, this mechanism requires that all the active sites cleave with high efficiency. This mechanism thus seems to be inconsistent with the formation of the largest products, which would require a relatively high probability that one-third or one-half of active sites failed to cleave their substrates. The requirement for cleavage at two adjacent active sites is also inconsistent with previous work indicating that the peptide size distribution is not altered by partial inactivation of the ClpP active sites (*8*).

A Physical Model for a ClpP-Controlled Stepwise Translocation Mechanism. While the kinetic and product size distribution results presented here support a mechanism in which substrate translocation occurs in discrete steps, the specific physical basis for these steps remains open to debate. The similarity in product size distributions for ClpAP- and ClpP-catalyzed caseinolysis suggests that, like the ClpAP-catalyzed reaction (*36*), the ClpP-catalyzed reaction proceeds via processive translocation of the polypeptide substrate. Although direct proof that the polypeptide enters the ClpP pore in discrete steps remains to be established, this proposal provides an economical explanation for the processivity and size distribution data presented here. While it is not yet clear how stepwise translocation might be coordinated in the absence of an ATPase, the crystal structure of ClpP may provide a useful starting point for thinking about possible mechanisms, since it shows the arrangement of the active sites and substrate binding sites. First, the spacing between the active sites may help determine the size of the steps. The crystal structure of ClpP indicates a spacing of approximately 7−8 amino acids between the active sites (*17, 18*), consistent with the spacing between the Gaussian components. In addition, the active sites of each heptameric ring are connected via a substrate-binding groove containing the S and S′ pocket sites (*37*). Each active site is expected to act as a relatively high affinity binding site due to the presence of these substrate binding regions (*17, 18, 37*). Taking into account these structural features, we can propose a physical model for processive translocation that accounts for processive proteolysis and product size control by ClpP via switches in binding affinity that are coupled to active site occupancy and peptide bond hydrolysis (Figure 7).

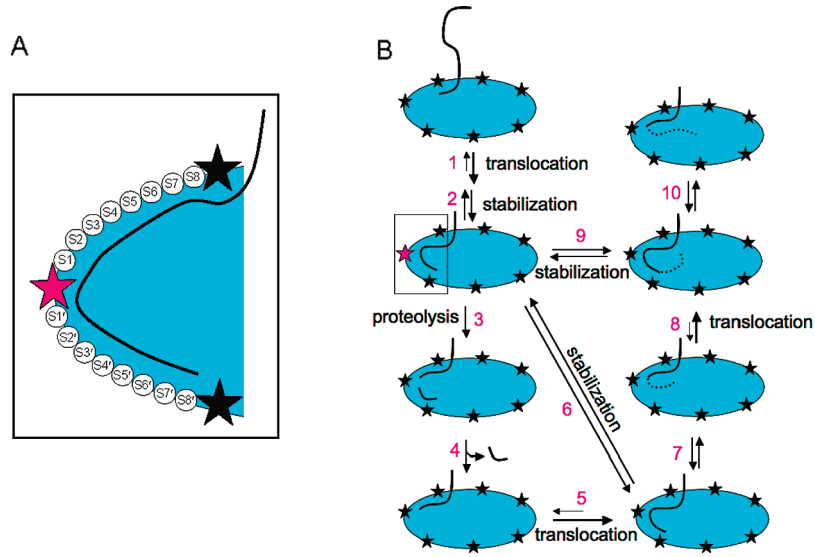

FIGURE 7: Speculative model for the ClpP-controlled stepping mechanism. Depicted in blue is a ring of active sites from one ClpP heptameric unit. The active sites are represented as stars and are connected via the substrate binding groove. (A) Close-up view of the active site binding region boxed in panel B. The S1−S8 and S1′−S8′ binding sites of one active site (depicted in red) are shown. (B) After the substrate binds to ClpP, it translocates via diffusion into the active site region (step 1). Once the substrate binds completely to an active site (i.e., to all the S and S′ binding sites), the interaction between substrate and enzyme is stabilized (step 2), leading to a high-affinity binding state from which proteolysis occurs (step 3). Proteolysis produces an ∼8-amino acid peptide product in the S′ site. [To illustrate this mechanism, we assume that translocation proceeds from the C-terminus to the N-terminus (*36*), placing the smaller product at the S′ site.] After proteolysis and product release (step 4), the substrate−enzyme binding affinity is lowered, and a translocation step can once again occur (step 5). This translocation step can be followed by stabilization (step 6) to the high-affinity binding state (from which proteolysis occurs), or the substrate can dissociate (step 7) before stabilization. Dissociation can be followed by an additional translocation step (step 8). After this step, the enzyme again partitions between stabilization followed by proteolysis (steps 9 and 3) and dissociation (step 10). Proteolysis after this second translocation step (step 8) will lead to a peptide product ∼16 amino acids in length.

In the proposed model (Figure 7), tight binding (i.e., complete binding to both the S and S′ pocket sites) is necessary for efficient proteolysis (Figure 7, step 2). Therefore, once a free segment of peptide binds tightly to both the S and S′ pockets of an active site, peptide bond hydrolysis occurs (Figure 7, step 3), generating a small (∼8-amino acid) product at the S′ site and leaving the larger product at the S site. Following hydrolysis, the affinity of both products is assumed to decrease, allowing them to leave their respective sites. Rapid release of the smaller product leaves the S′ site open (Figure 7, step 4). The equilibrium for productive translocation of the remaining protein substrate is favorable, since translocation causes both the S and S′ sites to be occupied. A translocation step can thus occur (Figure 7, step 5). Translocation is assumed to occur through essentially one-dimensional diffusion through the substrate binding groove, since that mode of transport would maximize favorable enzyme−substrate contacts during translocation. The translocation step can then be followed by tight binding of the translocated substrate to the S and S′ sites (Figure 7, step 6), leading to another round of proteolysis. Alternatively, if stabilization at the S′ site fails to occur rapidly enough compared to release of the translocated segment from that site (Figure 7, step 7), a second translocation step can take place before the next peptide hydrolysis reaction (Figure 7, step 8). If stabilization at the S′ site (Figure 7, step 9) again fails to occur rapidly enough compared to release of the translocated segment from that site (Figure 7, step 10), a third translocation step can take place before proteolysis, etc. This mechanism is similar to the "Brownian ratchet" mechanisms that have previously been proposed for classical motors (*38*).

The proposed model accounts for processive proteolysis and the generation of peptide products with average lengths at integral multiples of 7−8 amino acids. In the proposed model, the irreversible peptide bond cleavage and product release steps ensure that translocation is processive and unidirectional by driving the catalytic cycle in a single direction. The step size of 7−8 amino acids is determined by the size of the peptide binding sites in the protease active site (*37*), with the assumption that once both the S and S′ peptide binding sites are completely occupied, the substrate binds tightly, allowing proteolysis to occur. To the extent that the switch to tight binding is incompletely coupled to the complete occupancy of the peptide binding sites, the step size will be variable, as observed experimentally. When part of the substrate fails to bind tightly before a second translocation event can occur, the result is an increase in product length of 7−8 residues; each additional translocation event extends the product length by an additional increment of 7−8 residues. Further experimental work will be required to test this model. However, it has the advantage of accounting for existing results without requiring amide bond hydrolysis to drive large conformational changes in ClpP, a possibility that structural studies suggest is unlikely (*39*).

The mechanism described above is also consistent with previous reports indicating that the size distribution of peptide products is unaltered by inactivation of 70% of the active sites in ClpP (*8*). Unlike the molecular ruler mechanism, this mechanism requires only one functional active site in the chamber to achieve processivity. Assuming that cleavage products can dissociate rapidly and exit the chamber, rather than rebinding to another active site, the mechanism in Figure 7 predicts that partial inactivation will not change the size

distribution of products, since the translocating substrate interacts with only a single active site. Of course, the presence of multiple active sites is expected to accelerate the rate of the initial productive encounter between the substrate and an active site, consistent with the observation that covalent modification of 70−90% of the active sites does decrease the steady-state reaction rate (*8, 20*).

In the ClpAP complex, the conformational changes that drive translocation through the ClpP central pore may be coupled to the conformational changes that drive ClpA-catalyzed substrate translocation through the ClpA central pore (*40*). ClpA by itself can translocate substrates at rates much faster than those achieved by ClpP. However, the similarity between the product size distributions observed for ClpAP and ClpP alone suggests that ClpA does not change the elementary events that mediate translocation of a substrate through ClpP. Coordination of ClpA and ClpP conformational changes would allow ClpA to accelerate translocation through ClpP without changing the basic ClpP mechanism. Ample experimental evidence of conformational coupling between the protease and ATPase components of Clp proteases exists (*41*−*43*). In particular, the ClpP N-terminus may act to transduce conformational changes in ClpA to ClpP. The ClpP N-terminal domain is necessary for interaction with ClpA (*35, 44*), and the binding of ClpA causes the ClpP N-terminus to leave the central pore of the complex (L. D. Jennings et al., *Biochemistry*, in press). The presence or absence of the N-terminus in the ClpP central pore also appears to have a profound influence on the reactivity of the active site serine (L. D. Jennings et al., *Biochemistry*, in press), even though these regions of the complex are separated by tens of angstroms (*17*). The catalytic cycle proposed for ClpP-mediated translocation may thus be tightly coupled to the rapid conformational changes involved in ClpA-mediated translocation (*36, 40, 45*), allowing fast processive proteolysis only when both components are present.

These results may also provide insights into the mechanisms of other ATP-dependent proteases. The eukaryotic proteasome has been shown to processively degrade protein substrates in the absence of its ATPase binding partner (*21*), and the size distribution of its peptide products exhibits multiple peaks (*12*). This work provides analytical tools for evaluating mechanisms for proteasome-catalyzed processive proteolysis. Deconvolution of size-exclusion chromatograms to provide size distributions could, in principle, allow additional testing of the proposed filter mechanism (*10*) and alternative mechanisms. Further investigation of these mechanisms may help provide new insights into the important question of how epitope peptides are generated in the immune system.

ACKNOWLEDGMENT

We thank Dr. Bob Sauer, Dr. Tania Baker, and Dr. Søren Molin for donating plasmids; Mary Lee of the Sauer laboratory for purification advice; Dr. Barbara Imperiali for generously providing the use of the HPLC instrument; and Dr. Pete Wishnok and Dr. Steve Tannenbaum for use of their mass spectrometry facility.

SUPPORTING INFORMATION AVAILABLE

Supplementary methods detailing the tryptic and chymotryptic digests of BSA and ClpA, a comparison of the caseinolytic activity of ClpP purified from two different *Escherichia coli* strains [SG1146GaBL21(DE3) and DH5α], ClpAP-derived GFP-ssrA peptide product size-exclusion chromatogram, and observed and expected MALDI number distributions from chymotrypsin and trypsin digests of BSA and ClpA. This material is available free of charge via the Internet at http://pubs.acs.org.

REFERENCES

1. Gottesman, S., Maurizi, M. R., and Wickner, S. (1997) Regulatory subunits of energy-dependent proteases. *Cell 91*, 435–438.
2. Neuwald, A. F., Aravind, L., Spouge, J. L., and Koonin, E. V. (1999) AAA+: A class of chaperone-like ATPases associated with the assembly, operation, and disassembly of protein complexes. *Genome Res. 9*, 27–43.
3. Ogura, T., and Wilkinson, A. J. (2001) AAA+ superfamily ATPases: Common structure-diverse function. *Genes Cells 6*, 575–597.
4. Gottesman, S. (2003) Proteolysis in bacterial regulatory circuits. *Annu. Rev. Cell Dev. Biol. 19*, 565–587.
5. Baker, T. A., and Sauer, R. T. (2006) ATP-dependent proteases of bacteria: Recognition logic and operating principles. *Trends Biochem. Sci. 31*, 647–653.
6. Sauer, R. T., Bolon, D. N., Burton, B. M., Burton, R. E., Flynn, J. M., Grant, R. A., Hersch, G. L., Joshi, S. A., Kenniston, J. A., Levchenko, I., Neher, S. B., Oakes, E. S. C., Siddiqui, S. M., Wah, D. A., and Baker, T. A. (2004) Sculpting the proteome with AAA+ proteases and disassembly machines. *Cell 119*, 9–18.
7. Licht, S., and Lee, I. (2008) Resolving individual steps in the operation of ATP-dependent proteolytic molecular machines: From conformational changes to substrate translocation and processivity. *Biochemistry 47*, 3595–3605.
8. Choi, K. H., and Licht, S. (2005) Control of peptide product sizes by the energy-dependent protease ClpAP. *Biochemistry 44*, 13921–13931.
9. Kisselev, A. F., Akopian, T. N., and Goldberg, A. L. (1998) Range of sizes of peptide products generated during degradation of different proteins by archaeal proteasomes. *J. Biol. Chem. 273*, 1982–1989.
10. Kisselev, A. F., Akopian, T. N., Woo, K. M., and Goldberg, A. L. (1999) The sizes of peptides generated from protein by mammalian 26 and 20S proteasomes: Implications for understanding the degradative mechanism and antigen presentation. *J. Biol. Chem. 274*, 3363–3371.
11. Lun, D. S., Jennings, L. D., Koetter, R., Licht, S., and Médard, M. (2007) An information-based computational technique for estimation of chromatographic peak purity. *J. Chem. Inf. Model. 47*, 1973–1978.
12. Kohler, A., Cascio, P., Leggett, D. S., Woo, K. M., Goldberg, A. L., and Finley, D. (2001) The axial channel of the proteasome core particle is gated by the Rpt2 ATPase and controls both substrate entry and product release. *Mol. Cell 7*, 1143–1152.
13. Nishii, W., and Takahashi, K. (2003) Determination of the cleavage sites in SulA, a cell division inhibitor, by the ATP-dependent HslVU protease from *Escherichia coli*. *FEBS Lett. 553*, 351–354.
14. Nishii, W., Maruyama, T., Matsuoka, R., Muramatsu, T., and Takahashi, K. (2002) The unique sites in SulA protein preferentially cleaved by ATP-dependent Lon protease from *Escherichia coli*. *Eur. J. Biochem. 269*, 451–457.
15. Nishii, W., Suzuki, T., Nakada, M., Kim, Y. T., Muramatsu, T., and Takahashi, K. (2005) Cleavage mechanism of ATP-dependent Lon protease toward ribosomal S2 protein. *FEBS Lett. 579*, 6846–6850.
16. Lowe, J., Stock, D., Jap, R., Zwickl, P., Baumeister, W., and Huber, R. (1995) Crystal structure of the 20S proteasome from the archaeon *T. acidophilum* at 3.4 Å resolution. *Science 268*, 533–539.
17. Wang, J. M., Hartling, J. A., and Flanagan, J. M. (1997) The structure of ClpP at 2.3 Å resolution suggests a model for ATP-dependent proteolysis. *Cell 91*, 447–456.

18. Wang, J., Hartling, J. A., and Flanagan, J. M. (1998) Crystal structure determination of *Escherichia coli* ClpP starting from an EM-derived mask. *J. Struct. Biol. 124*, 151–163.
19. Wenzel, T., Eckerskorn, C., Lottspeich, F., and Baumeister, W. (1994) Existence of a molecular ruler in proteasomes suggested by analysis of degradation products. *FEBS Lett. 349*, 205–209.
20. Thompson, M. W., Singh, S. K., and Maurizi, M. R. (1994) Processive degradation of proteins by the ATP-dependent Clp protease from *Escherichia coli*. Requirement for the multiple array of active sites in ClpP but not ATP hydrolysis. *J. Biol. Chem. 269*, 18209–18215.
21. Akopian, T. N., Kisselev, A. F., and Goldberg, A. L. (1997) Processive degradation of proteins and other catalytic properties of the proteasome from *Thermoplasma acidophilum*. *J. Biol. Chem. 272*, 1791–1798.
22. Bruckner, R. C., Gunyuzlu, P. L., and Stein, R. L. (2003) Coupled kinetics of ATP and peptide hydrolysis by *Escherichia coli* FtsH protease. *Biochemistry 42*, 10843–10852.
23. Nelson, D. L., and Cox, M. M. (2000) *Lehninger Principles of Biochemistry*, 3rd ed., Worth Publishers, New York.
24. Saffarian, S., Collier, I. E., Marmer, B. L., Elson, E. L., and Goldberg, G. (2004) Interstitial collagenase is a Brownian ratchet driven by proteolysis of collagen. *Science 306*, 108–111.
25. Kim, Y. I., Burton, R. E., Burton, B. M., Sauer, R. T., and Baker, T. A. (2000) Dynamics of substrate denaturation and translocation by the ClpXP degradation machine. *Mol. Cell 5*, 639–648.
26. Maurizi, M. R., Thompson, M. W., Singh, S. K., and Kim, S. H. (1994) Endopeptidase Clp: ATP-dependent Clp protease from *Escherichia coli*. *Methods Enzymol. 244*, 314–331.
27. Yakhnin, A. V., Vinokurov, L. M., Surin, A. K., and Alakhov, Y. B. (1998) Green fluorescent protein purification by organic extraction. *Protein Expression Purif. 14*, 382–386.
28. Rypniewski, W. R., Holden, H. M., and Rayment, I. (1993) Structural consequences of reductive methylation of lysine residues in hen egg-white lysozyme: An X-ray-analysis at 1.8 Å resolution. *Biochemistry 32*, 9851–9858.
29. Udenfriend, S., Stein, S., Bohlen, P., Dairman, W., Leimgruber, W., and Weigele, M. (1972) Fluorescamine: A reagent for assay of amino acids, peptides, proteins, and primary amines in the picomole range. *Science 178*, 871–872.
30. Silvestre, M. P. C., Hamon, M., and Yvon, M. (1994) Analysis of protein hydrolysates. 1. Use of poly(2-hydroxyethylaspartamide)-silica column in size-exclusion chromatography for the fractionation of casein hydrolysates. *J. Agric. Food Chem. 42*, 2778–2782.
31. Maurizi, M. R., Clark, W. P., Kim, S. H., and Gottesman, S. (1990) ClpP represents a unique family of serine proteases. *J. Biol. Chem. 265*, 12546–12552.
32. Akaike, H. (1974) A new look at statistical model identification. *IEEE Trans. Autom. Control 19*, 716–723.
33. Milton, J. S., and Arnold, J. C. (2003) *Introduction to probability and statistics: Principles and applications for engineering and the computing sciences*, 4th ed., McGraw-Hill, New York.
34. Sprangers, R., Gribun, A., Hwang, P. M., Houry, W. A., and Kay, L. E. (2005) Quantitative NMR spectroscopy of supramolecular complexes: Dynamic side pores in ClpP are important for product release. *Proc. Natl. Acad. Sci. U.S.A. 102*, 16678–16683.
35. Gribun, A., Kimber, M. S., Ching, R., Sprangers, R., Fiebig, K. M., and Houry, W. A. (2005) The ClpP double ring tetradecameric protease exhibits plastic ring-ring interactions, and the N termini of its subunits form flexible loops that are essential for ClpXP and ClpAP complex formation. *J. Biol. Chem. 280*, 16185–16196.
36. Reid, B. G., Fenton, W. A., Horwich, A. L., and Weber-Ban, E. U. (2001) ClpA mediates directional translocation of substrate proteins into the ClpP protease. *Proc. Natl. Acad. Sci. U.S.A. 98*, 3768–3772.
37. Kim, D. Y., and Kim, K. K. (2008) The structural basis for the activation and peptide recognition of bacterial ClpP. *J. Mol. Biol. 379*, 760–771.
38. Reimann, P. (2002) Brownian motors: Noisy transport far from equilibrium. *Phys. Rep. 361*, 57–265.
39. Szyk, A., and Maurizi, M. R. (2006) Crystal structure at 1.9 Å of *E. coli* ClpP with a peptide covalently bound at the active site. *J. Struct. Biol. 156*, 165–174.
40. Hinnerwisch, J., Fenton, W. A., Furtak, K. J., Farr, G. W., and Horwich, A. L. (2005) Loops in the central channel of ClpA chaperone mediate protein binding, unfolding, and translocation. *Cell 121*, 1029–1041.
41. Joshi, S. A., Hersch, G. L., Baker, T. A., and Sauer, R. T. (2004) Communication between ClpX and ClpP during substrate processing and degradation. *Nat. Struct. Mol. Biol. 11*, 404–411.
42. Martin, A., Baker, T. A., and Sauer, R. T. (2007) Distinct static and dynamic interactions control ATPase-peptidase communication in a AAA+ protease. *Mol. Cell 27*, 41–52.
43. Hinnerwisch, J., Reid, B. G., Fenton, W. A., and Horwich, A. L. (2005) Roles of the N-domains of the ClpA unfoldase in binding substrate proteins and in stable complex formation with the ClpP protease. *J. Biol. Chem. 280*, 40838–40844.
44. Bewley, M. C., Graziano, V., Griffin, K., and Flanagan, J. M. (2006) The asymmetry in the mature amino-terminus of ClpP facilitates a local symmetry match in ClpAP and ClpXP complexes. *J. Struct. Biol. 153*, 113–128.
45. Farbman, M. E., Gershenson, A., and Licht, S. (2007) Single-molecule analysis of nucleotide-dependent substrate binding by the protein unfoldase ClpA. *J. Am. Chem. Soc. 129*, 12378–12379.
46. Siuzdak, G. (2003) *The expanding role of mass spectrometry in biotechnology*, MCC Press, San Diego.

BI801101P